Published in final edited form as:
Traffic. 2013 July ; 14(7): 823–838. doi:10.1111/tra.12076.

A sorting nexin 17-binding domain within the LRP1 cytoplasmic tail mediates receptor recycling through the basolateral sorting endosome

Pamela Farfán[1,2,*], **Jiyeon Lee**[3,*], **Jorge Larios**[1,2], **Pablo Sotelo**[1], **Guojun Bu**[4,#], and **María-Paz Marzolo**[1,2,#]

[1]Laboratorio de Tráfico Intracelular y Señalización, Departamento de Biología Celular y Molecular, Facultad de Ciencias Biológicas, Pontificia Universidad Católica de Chile

[2]Millenium Nucleus in Regenerative Biology (MINREB), Pontificia Universidad Católica de Chile

[3]Diabetic Cardiovascular Disease Center and Department of Medicine, Washington University, St. Louis, MO 63110, USA

[4]Department of Neuroscience, Mayo Clinic, Jacksonville, Florida 32224, USA

Abstract

Sorting nexin 17 (SNX17) is an adaptor protein present in EEA1-positive sorting endosomes that promotes the efficient recycling of low-density lipoprotein receptor-related protein 1 (LRP1) to the plasma membrane through recognition of the first NPxY motif in the cytoplasmic tail of this receptor. The interaction of LRP1 with SNX17 also regulates the basolateral recycling of the receptor from the basolateral sorting endosome (BSE). In contrast, megalin, which is apically distributed in polarized epithelial cells and localizes poorly to EEA1-positive sorting endosomes, does not interact with SNX17, despite containing three NPxY motifs, indicating that this motif is not sufficient for receptor recognition by SNX17. Here, we identified a cluster of 32 amino acids within the cytoplasmic domain of LRP1 that is both necessary and sufficient for SNX17 binding. To delineate the function of this SNX17-binding domain, we generated chimeric proteins in which the SNX17-binding domain was inserted into the cytoplasmic tail of megalin. This insertion mediated the binding of megalin to SNX17 and modified the cell surface expression and recycling of megalin in non-polarized cells. However, the polarized localization of chimeric megalin was not modified in polarized MDCK cells. These results provide evidence regarding the molecular and cellular mechanisms underlying the specificity of SNX17-binding receptors and the restricted function of SNX17 in the BSE.

Keywords

SNX17; sorting endosome; recycling endosome; megalin; LRP1; polarized cells

Introduction

Sorting Nexin 17 (SNX17) is a member of the sorting nexin (SNX) family, characterized by the presence of a phox (PX) domain (1), which localizes SNXs to intracellular vesicles

[#]Corresponding Authors: Dr. María-Paz Marzolo, Departamento de Biología Celular y Molecular, Facultad de Ciencias Biológicas, Pontificia Universidad Católica de Chile, Casilla 114-D, Santiago, Chile. Telephone: 56-2-6862112; Fax 56-2-2229995; mmarzolo@bio.puc.cl. Dr. Guojun Bu, Department of Neuroscience, Mayo Clinic, Jacksonville, Florida 32224, USA; Bu.Guojun@mayo.edu.
[*]Both authors contributed equally to this work

through interactions with specific phosphatidylinositol phosphates (2, 3), and an atypical band, 4.1/exrin/radixin/moesin (FERM) domain, responsible for cargo recognition (4, 5). Similar to many SNXs, SNX17 is localized to early endosomes (5–7). Many studies have demonstrated that SNX17 regulates the endocytic trafficking of several LDLR family members, including LDLR and LRP1, through NPxY motifs in their cytoplasmic domains (5–7). These motifs are also required for binding to SNX17 in the LDLR family members ApoER2 and LRP1B (7) (van Kerkhof et al., data not shown). In addition, our work has shown that amyloid precursor protein (APP), which is processed to generate Alzheimer's toxic amyloid-β (Aβ) peptides, also binds to SNX17 through the NPxY motif (8). Recent studies have demonstrated that β1-integrin binds to SNX17 through the NPxY motif and that this interaction controls the lysosomal degradation and recycling of integrins (9, 10). Therefore, it is clear that the NPxY motif is required for binding to SNX17, specifically to the FERM domain. However, the NPxY motif alone is not sufficient for binding to SNX17, as megalin, also known as LRP2, contains three NPxY motifs but does not interact with SNX17 (7). Similarly, the C-terminal half of the LRP1 tail does not interact with SNX17, although it contains an NPxY motif similar to the membrane-proximal motif, which binds SNX17 (5). These findings indicate that the NPxY motif is necessary, but not sufficient for binding to SNX17.

Although short linear *binding motifs*" mediate protein-protein interactions, recent findings raise the question of whether these 4–6-amino acid-long motifs are sufficient for binding to specific partners. For example, the clathrin motif box, which is typically referred to as Lφpφ(−) (φ for bulky hydrophobic, p for polar, and (−) for negatively charged residues), contains a number of variants of clathrin-binding sites, including a nonpolar residue inserted between positions 4 and 5 of the Lφpφ(−) motif and LLDLL (no charge at position 5) (11). Furthermore, in addition to SNX17, an NPxY motif is also required for binding to several other cytoplasmic adaptor proteins (5, 8, 12–14). Therefore, we reasoned that the NPxY motif is not sufficient for SNX17 binding to receptor tails.

We hypothesized that the amino acids neighboring the NPxY motif are required for the specificity and function of SNX17 binding. Burden et al. showed that mutations in the amino acids flanking the NPxY motif disrupt the binding of LDLR to SNX17 (6). Similar mutations in the cytoplasmic domain of P-selectin also inhibit the interaction between P-selectin and SNX17 (15). We have also previously demonstrated that mutation of several residues downstream of the IxNPxY motif significantly reduce the ability of LRP1 to bind SNX17 (5). We examined our hypothesis via serial deletion and amino acid substitution analyses and identified a *SNX17-binding domain*, which is both necessary and sufficient for binding to SNX17.

SNX17 is localized to the EEA1-positive early/sorting endosomes (6, 9). These endosomes are traffic stations in which the decision to travel to the plasma membrane, common recycling endosome (CRE), degradation pathway, or trans-Golgi network (TGN) is made (16–21). Plasma membrane receptors, such as LDLR family members, exhibit highly active endocytic/recycling behavior and enter this compartment many times during their lifetimes. Endocytic recycling has long been considered as a default pathway. However, recent evidence suggests that this signal-mediated recycling pathway also involves the cellular machinery (5, 22–24); this mechanism has been best described (though not exclusively) at the level of the CRE (25–28). In this context, the need for SNX17-binding motifs to achieve efficient recycling of receptors, such as LRP1 (5, 29), indicates that the recycling process at the early/sorting endosome is also signal mediated. Moreover, recent data (29) indicate that recycling from an early endosomal compartment in polarized cells, including hippocampal neurons and the epithelial cell line MDCK, is more dependent on the SNX17-binding site than in non-polarized cells (5). The nature of the early/sorting endosomes in polarized

epithelial cells is different from that in non-polarized cells (30). Specifically, these compartments include different apical and basolateral early/sorting endosomes, apical sorting endosome (ASE) and basolateral sorting endosome (BSE), respectively (31). In MDCK cells, SNX17 primarily co-localizes with EEA1 in endosomes (29), which correspond to a subpopulation of basolateral early endosomal compartments lacking apical proteins, such as endotubin (30), indicating that apical recycling proteins might not require SNX17.

In this study, we produced a detailed description of the SNX17-binding domain present in the cytoplasmic domain of LRP1. We also characterized the functional impact of binding to SNX17 on the trafficking and distribution of megalin, an apical receptor that does not interact with SNX17 (7, 32). We showed that the presence of the SNX17-binding domain not only mediated binding between megalin and SNX17 but also altered the intracellular trafficking of this protein, particularly regarding the recycling and cell surface expression of megalin in non-polarized cells. However, chimeric megalin remained localized to the apical membrane, displaying a low degree of co-localization with endosomal compartments positive for SNX17 compared with LRP1 in polarized MDCK cells. This result suggests that the role of SNX17 is restricted to basolateral cargo recycling through the BSE in polarized epithelial cells, despite showing interactions with the target receptor.

Results

The IxNPxY motif is not sufficient for binding to SNX17

The IxNPxY motif, which is the membrane-proximal NPxY motif in the cytoplasmic domain of LRP1, is required for the binding of LRP1 to SNX17 (5). To examine whether the IxNPxY motif itself is sufficient for this interaction, we performed GST pull-down assays (Fig. 1B–D) using several receptor tail mutants. Figure 1A shows a schematic diagram of the full-length (construct “a”) and deletion mutants (constructs “b–f”) of the LRP1 tail, which were incubated with lysates from U87 cells stably expressing full-length mycSNX17. GST alone served as a negative control. As previously shown, the C-terminal half of the LRP1 tail (T44-100) (construct “b”) does not bind to SNX17. Addition of the IGNPTY motif to the N-terminal half of T44-100 did not significantly alter its ability to bind SNX17 (construct “c”). Furthermore, replacing the FTNPVY motif with IGNPTY in the T44-100 construct also had no effect (construct “d”). Therefore, we concluded that although the IGNPTY motif is necessary for binding to SNX17, it is not sufficient and is likely dependent on flanking sequences (Fig. 1B).

Interestingly, a mutant construct in which the membrane-proximal IGNPTY motif was replaced with FTNPVY (construct “f”) exhibited stronger binding than its wild-type counterpart (T4-53, construct “e”) (Fig. 1B). This result indicates that phenylalanine serves as a motif that mediates a stronger interaction between LRP1 and SNX17 than isoleucine and that the flanking regions could provide a better environment for the presentation of this motif.

The area spanning amino acids 14–45 of the LRP1 cytoplasmic domain is the minimal region required for SNX17 binding

The insufficiency of the short IxNPxY motif for binding to SNX17 prompted us to identify the region of the cytoplasmic domain of LRP1 required for interaction with SNX17. We examined serial deletion constructs of the GST-LRP1 tail based on their interaction with SNX17 (Fig. 1A, constructs “e, g–I”). Truncation of the LRP1 tail at amino acids 46–100 (construct “h”) did not disturb LRP1 binding to SNX17, while truncation at amino acid 41 (construct “I”) completely disrupted this interaction (Fig. 1C). Similarly, at the N-terminus,

a deletion mutant consisting of amino acids 14–45 of the LRP1 tail (construct “j”) retained binding to SNX17, while the “k” construct, comprised of amino acids 24–45, did not (Fig. 1C). Therefore, amino acids 14–45 of the LRP1 cytoplasmic domain (T14-45), referred to as the SNX17-binding domain, are sufficient for SNX17 binding.

To further analyze the role of amino acids 41–45 (GGLLD) in the interaction between LRP1 and SNX17, the leucine and aspartic acid residues in this sequence were mutated to alanines (compare construct “h” with “l” and “m”). These mutations reduced the ability of the LRP1 tail to bind SNX17, whereas double glycine mutations did not (construct “n”, Fig. 1D). Surprisingly, mutating all five amino acids to alanine did not completely block the interaction between the LRP1 tail and SNX17 (construct “o”), whereas deleting these amino acids (construct “i”) abolished this interaction, suggesting that the presence of any five amino acids in the C-terminal region of the NPXY motif might contribute to SNX17 binding.

Amino acids both upstream and downstream of the IxNPxY motif contribute to SNX17 binding

The fact that SNX17 only binds to the membrane-proximal NPxY motif prompted an examination of the contribution of the adjacent amino acids. For simplification, we refer to the regions adjacent to each NPxY motif as A, B, C, and D. As shown in Figure 2A, regions C and/or D in the T44-100 construct (Fig. 2A construct “a”) were replaced with regions A and/or B (Fig. 2A construct “b–d”). Construct “b” bound weakly to SNX17, but construct “c” bound strongly (Fig. 2B). T44-100 construct “d”, in which the C and D regions were replaced with A and B, interacted with SNX17 as strongly as construct “g”, indicating that regions A and B contribute synergistically to SNX17 binding in this context. The contribution of region A appears to be context dependent. When co-expressed with region D, this region mediated the binding of SNX17 in the context of the FTNPVY sequence from T44-100 (construct “c”, second half of the LRP1 tail), but not in the context of the first half of the LRP1 tail (construct “e). Within the first half of the LRP1 tail, region A absolutely required the presence of region B for efficient binding (construct “g”). However, the fact that construct “h” did not bind to SNX17 also suggests that region B alone is not sufficient for SNX17 binding, and both regions A and B contribute greatly to SNX17 binding.

Acidic amino acid residues downstream of the IxNPxY motif are required for the efficient binding of LRP1 to SNX17

The SNX17-binding domain in the LRP1 tail (T14-45) contains amino acids with characteristics that could be important determinants of protein-protein interactions. A comparison of the amino acid residues in the receptor tails that contribute to SNX17 binding revealed that region B in the membrane-proximal IxNPxY motif (^{30}KMYEGGEPDD^{39}) is rich in acidic residues (glutamate and aspartate), which are not present near the membrane-distal NPxY motif in the LRP1 tail (Fig. 3A). A similar amino acid stretch is found in the cytoplasmic tails of LDLR and ApoER2 (Fig. 3A), which both bind to SNX17 ((7) and Sotelo et al., manuscript in preparation). Because the polarity or charge of amino acid side chains strongly affects protein-protein interactions, we reasoned that these negatively charged amino acids adjacent to the IxNPxY motif could be critical for the role of region B in LRP1 binding to SNX17.

To test this hypothesis, three mutant constructs with different mutations downstream of the IxNPxY motif were generated (Fig. 3B). Changing the acidic residues in region B to alanines (Fig. 3B construct “c”) significantly disrupted the interaction between LRP1 and SNX17, and replacing the negatively charged residues with positively charged arginine residues (Fig. 3B construct “b”) completely prevented LRP1 from binding to SNX17 (Fig.

3C). Therefore, the negatively charged residues downstream of the IxNPxY motif (region B) participate in the binding of LRP1 to SNX17. Although further characterization must be performed to determine the roles of individual residues, these results suggest that the acidic residues within the SNX17-binding domain are important for the interaction between LRP1 and SNX17.

A chimeric megalin receptor containing the SNX17-binding domain of LRP1 interacts with SNX17

To further confirm whether the SNX17-binding domain of LRP1 is sufficient for SNX17 binding, we generated a megalin tail construct containing the SNX17-binding domain. The cytoplasmic domain of megalin contains three NPxY motifs, but megalin does not bind to SNX17 (7). Accordingly, a GST-megalin tail construct also does not bind to SNX17 (Fig. 4B, lane c). In contrast, the chimeric construct containing the wild-type SNX17-binding domain (IxNPTY) interacted strongly with SNX17, whereas a mutant (IxNPTA) bound weakly (Fig. 4B, constructs “d” and “e”). The SNX17-binding domain was inserted into the region after residue 13 of the megalin tail (Fig. 4A, constructs “d” and “e”) to maintain a relative position in the transmembrane domain similar to the position in LRP1. Replacing the first NPXY motif of megalin with the SNX17-binding domain yielded similar results (Fig. S2 A, B), confirming that the presence of the SNX17-binding domain of LRP1 is sufficient for binding to SNX17.

The presence of the SNX17-binding domain increases the cell surface expression of megalin and renders a different endosomal distribution

SNX17 enhances the recycling of LRP1, but does not affect receptor internalization (5). To analyze whether this domain affects the trafficking of megalin, we generated chimeric minimegalin receptors (Fig. 5 A, B). Minimegalin has previously been shown to behave similarly to the endogenous full-length receptor regarding its internalization, recycling, phosphorylation, and apical distribution (23, 33). Wild-type mMeg (mMeg-1) and chimeric receptors containing an intact or mutant SNX17-binding domain (mMeg-2 and mMeg-3, respectively) were expressed in HEK293 cells, and the ratio of cell surface to total receptors was analyzed through flow cytometry. The presence of the SNX17-binding domain in the megalin cytoplasmic tail (mMeg-2) significantly increased the expression of this receptor at the cell surface (Fig. 5C). However, the mutant chimera mMeg-3 showed cell surface expression similar to mMeg-1, indicating that an intact IxNPxY motif is required to increase the cell surface expression of megalin. Knockdown of SNX17 expression (Fig. S1A) reduced the cell surface expression of the mMeg-2. (Fig. 5C) but did not affect the cell surface levels of mMeg-1, as this protein did not bind SNX17.

The increased cell surface expression of mMeg-2 could reflect more efficient trafficking from the early endosome, where SNX17 functions, directly to the plasma membrane and/or indirectly through the recycling endosome. To examine this possibility, we compared the intracellular post-endocytic steady-state distribution of different receptors in HEK293 cells using a continuous internalization protocol for the receptor ligand RAP and determined either the distribution of this protein compared with the transferring receptor or the colocalization of RAP with the endosomal recycling marker Rab4. Cells were incubated with GST-RAP for 30 min, followed by an additional 75-min incubation with GST-GFP-RAP. At the end of the internalization assay, the ligands at the cell surface were acid stripped, and the internalized RAP was visualized based on GFP fluorescence. The localization of the transferrin receptor (TfR) indicates the recycling compartments. Figure 6A shows the three major distribution patterns obtained for the internalized receptor under these conditions: a vesicular pattern including partial co-localization with TfR, both vesicular and perinuclear staining, and a predominant perinuclear distribution with clear TfR

co-localization. More than 100 cells expressing each receptor were counted for each experiment, and the results corresponding to three independent experiments performed using wild-type and SNX17 KD HEK293 cells are shown in Figures 6B and C (see also Table S1 for detailed results). A significant proportion (40%) of mMeg-2 displayed perinuclear staining, whereas the control minireceptor protein, mMeg-1, primarily displayed a peripheral vesicular pattern (57%), with no more than 12% perinuclear staining being observed. Knockdown of SNX17 abrogated the differential distribution of GST-GFP-RAP in mMeg-2-expressing cells (Fig. 6C and Table S1). These results indicate that binding to SNX17 increases the localization of megalin to perinuclear recycling endosomal compartments.

To complement these observations and confirm these results, we determined the colocalization of the different receptors with the fast-endosomal recycling marker Rab4, which also localizes with SNX17 (7). Figure 7A, shows representative images of confocal sections displaying the maximum receptor signal in the endocytic pathway (using the same protocol used in Fig. 6) and Rab4-mCherry. Quantification of the observed colocalization pattern indicated that more than 25% of mMeg-2 is present in Rab4-recycling endosomes, whereas less than 20% colocalization was observed for both mMeg-1 and mMeg-3 (Fig. 7B). Thus, consistent with previous results (Fig. 6C), the increased presence of mMeg-2 in the recycling endosomes depends on the expression of SNX17 (Fig. 7B).

We also analyzed the total population of cells exhibiting different percentages of receptors present in Rab4-recycling endosomes. Figure 7C shows that approximately 50% of the cells expressing mMeg-1 showed low (less than 15%) colocalization of the receptor and Rab4, whereas in the remaining cells, 15–30% colocalization was observed. This distribution pattern was significantly different for cells expressing mMeg-2, which binds SNX17: in the majority of these cells (more than 76%), the receptor was present in 15–30% of Rab4 structures, and approximately 11% of these cells showed high (more than 30%) colocalization. In contrast, in the majority of cells expressing mMeg-3, the receptor colocalized poorly with Rab4 (less than 15% of the receptor colocalized), and we did not observe cells in which more than 30% of the receptor was present in recycling Rab4-endosomes. Interestingly, the distribution pattern observed in cells expressing mMeg-2 was SNX17 dependent (Fig. 7D), as in the majority of SNX17 KD cells, less than 15% of the receptor was present in recycling endosomes. Similar results were observed in SNX17 KD cells expressing mMeg-1 and mMeg-3, in which receptor colocalization with Rab4 was not significantly modified upon SNX17 silencing. Overall, these results (Figs, 5–7) indicate that mMeg-2 is more frequently present in recycling compartments and at the cell surface, indicating more efficient recycling in the presence of SNX17.

Based on its more efficient recycling, as shown for integrins (9), mMeg-2 could be more stable and less likely targeted for degradation than receptors that do not bind SNX17. To confirm this possibility, both the steady state and turnover of the different receptors were examined in HEK293 cells. A representative result of three similar experiments is shown in Figure 8. The half-life and steady-state levels of the receptors were determined in cells that were metabolically labeled with [^{35}S] methionine/cysteine, as described in the Methods. The immunoprecipitates obtained after 9 and 18 h chase periods indicated the existence of degradation conditions (Fig. 8A). We observed a small, but significant reduction in the levels of mMeg-3 compared with mMeg-2 after an 18 h chase (Fig. 8B). In some experiments, we also found that the levels of mMeg-2 were significantly increased compared with wild-type minimegalin (mMeg-1) after an 18 h chase (not shown). However, comparing the steady-state levels of the immature receptor (low MW band) with those of the mature receptor revealed a consistent small, but significant, increase in the mature/immature receptor ratio when mMeg-2 and mMeg-3 were compared (Fig. 8C), revealing that the degradation of mMeg-2 was reduced. Overall, these results indicate that the presence of a

SNX17-binding domain has a small effect in the half-life of megalin, in contrast with the more relevant role of the IxNPxY motif in LRP1 (5) and the role of SNX17 in β1-integrin retrieval from lysosomes (9, 10).

The presence of the SNX17-binding domain increases the localization of megalin to EEA1 endosomes but does not alter the apical distribution of the receptor in polarized MDCK cells

In polarized cells, the basolateral protein LRP1 recycles to the basolateral membrane from the BSE, which is positive for EEA1 and SNX17, in a manner that is strictly dependent on the integrity of the first NPxY motif (29). Therefore, SNX17 would be expected to participate in the LRP1 basolateral sorting machinery in a post-endocytic step. In contrast, megalin, which is apically distributed in epithelial cells, should not recycle to the plasma membrane through BSE. To determine whether the presence of the SNX17-binding domain in the megalin tail alters the trafficking of this protein, we generated MDCK cells stably expressing different megalin minireceptors.

The cells were grown on filters until polarization to analyze the surface distribution of the membrane proteins, including minimegalin, via domain-specific biotinylation. At least three independent clones were analyzed for each construct. As shown in Figure 9, despite the presence of the insert within the megalin cytoplasmic tail, all of the minimegalins were predominantly apical. As a control to correct for polarization, the basolateral distribution of E-cadherin was also determined.

The apical sorting of megalin follows a direct pathway from the TGN (32). Therefore, although mMeg-2 interacts with SNX17 and is recycled in a SNX17-dependent fashion in non-polarized cells (Fig. 5 and 7), in polarized epithelial MDCK cells, the receptor recycles primarily through the ASE and/or from the CRE, and not from BSE, where SNX17 is located (29). We quantified the different megalin minireceptors present in EEA1-positive endosomal compartments, which are primarily basolateral in polarized epithelial cells (30). As controls, we also analyzed the localization of the minireceptor mLRP1 and the distribution of all of the constructs in SNX17 KD MDCK cells (see Table S2 for detailed results and Fig. S1B for the detection of SNX17 in control and SNX17-silenced MDCK cells). Considering the total amounts of the receptor present in the biosynthetic and endocytic pathways, in the cellular area positive for EEA1-endosomal structures (representing more than 96% of the total receptor content in the cell), approximately 18% of the mLRP1-positive structures co-localized with EEA1 (Fig. 10). In contrast, no more than 4.4% of mMeg-1 was localized in EEA1-positive structures. The presence of the SNX17-binding domain significantly increased the localization of mMeg-2 in EEA1-positive endosomes to 7.1%. ($p<0.05$ vs. mMeg-1). This localization was reduced to 3.9% for mMeg-3 (n.s. vs. mMeg-1). In SNX17-depleted cells, the percentage of mMeg-2 in EEA1 endosomes decreased to 3.5% ($p< 0.01$ vs. mMeg-2 in control cells), suggesting that the localization of chimeric megalin to this early endocytic compartment depends on SNX17 recognition. The distribution of mMeg-1 and mMeg-3 was not altered in the EEA1 endosomes when SNX17 was silenced. Representative images corresponding to the slices exhibiting the maximal amounts of the receptor and EEA1-positive structures also showed different degrees of co-localization in the control cells (Fig. 10B). These results indicate that the insertion of the SNX17-binding domain in the cytoplasmic tail of megalin slightly increases the localization of this protein in EEA1-positive endosomes, although to a lesser degree than LRP1, which primarily recycles through the BSE to the basolateral membrane (29). Therefore, the recycling of chimeric mMeg-2 would primarily occur from endosomal compartments devoid of SNX17, reflecting the maintenance of apical polarity observed for this chimeric receptor.

Discussion

Many studies have shown that short linear arrangements of amino acids in proteins referred to as “binding motifs” determine protein binding partners. Several adaptor proteins bind to the motif(s) present in the cytoplasmic domains of cell surface receptors and control the intracellular trafficking of those receptors. For example, Dab2 interacts with LDLR via the FxNPxY motif (34), which is conserved in the cytoplasmic domain of several LDLR family proteins. However, these binding motifs are not completely conserved, and variant motifs can occasionally retain binding ability (11, 35, 36). Moreover, the fact that not all proteins containing the consensus motif are functional and that only one of the duplicated motifs is responsible for binding suggests that several other factors contribute to protein-protein interactions (11). These factors could include intracellular localization and additional amino acid sequences that have thus far gone unrecognized.

Based on previous reports and studies addressing the interactions of LDLR and LRP1 with SNX17 (5, 6), we examined whether the NPxY motif is sufficient for SNX17 binding. We identified and characterized a 32-amino acid region comprising the NPxY motif as the *SNX17-binding domain* in the LRP1 tail, which is sufficient for binding to SNX17. The addition of this domain to the tail of megalin conferred a capacity for SNX17 binding and modified receptor trafficking, specifically the recycling of megalin, in a SNX17-dependent manner. Interestingly, however, the presence of the SNX17-binding domain in megalin did not significantly affect the stability of the receptor, in contrast with what is observed for natural SNX17-binding receptors, such as LRP1 (5), APP (8), and β1-integrins (9, 10). Wild-type megalin and the megalin minireceptor are slowly degraded, with a half-life of over 15 h (data not shown, Sandoval L., unpublished results from our lab). The factors controlling the half-life of megalin remain unknown; however, this mechanism is also likely to function in the chimeric forms of megalin, making it difficult to determine the role of the interaction with SNX17 as a determinant for the degradation pathway.

SNX17 binding is related to the trafficking and recycling of receptors and membrane proteins (5, 7, 9, 29), which are basolaterally distributed in polarized cells. In addition, in polarized cells, the requirement for the SNX17-binding site is more critical than in non-polarized cells for proper recycling (29). Thus, we examined whether the SNX17-binding domain present in the cytoplasmic domain of the basolateral recycling protein LRP1 would affect the distribution and trafficking of megalin, an apical receptor (32). The presence of this domain in two different positions within the megalin tail, in the form of mMeg-2 (Fig. 9) and mMeg-4 (Fig. S2C), did not alter the apical distribution of the receptors expressed in the kidney epithelial MDCK cell line, although the localization of these receptors to EEA1-positive endosomes was increased (Fig. 10 and Table S2). Compared with the distribution of LRP1, however, the percentage of the chimeric megalin receptors in the EEA1/basolateral endosome remained low, indicating that the presence of this domain does not modify the polarized distribution of megalin during its recycling. Notably, the insertion of a mutant SNX17-binding site also did not disrupt the apical sorting of megalin, indicating that the insertion of this domain *per se* did not alter the biosynthetic apical sorting signal and/or that if this signal was disrupted, then other recessive apical determinants present in the N-Glycosylated ectodomain of megalin and/or associated transmembrane-mediated lipid rafts (32) could be operating. These results further imply that the endosomal recycling capacity of SNX17 is restricted in polarized epithelial cells. The apical and basolateral endocytic pathways in polarized cells merge in the CRE, which is positive for both the AP-1B adaptor complex (25, 37) and rab8 GTPase (38, 39). From this compartment, some internalized apical proteins are directed to the Rab11-positive apical recycling endosome (ARE) and subsequently to the apical membrane, while basolateral internalized recycling proteins, such as LRP1 and LDLR, are directed to the basolateral plasma membrane, potentially through

the AP-1B adaptor complex (24, 29). Therefore, in polarized epithelial cells, SNX17 might not participate in the sorting of cargo from the CRE and/or the apical recycling compartments, which explains why the chimeric megalin containing the SNX17 domain remained in the apical membrane, as apical recycling would be unaffected. Overall, these results in MDCK cells reinforce the concept that in polarized epithelial cells, SNX17-mediated recycling might be limited to a subset of EEA1-positive basolateral endosomes, which would require receptor entry following internalization from the basolateral membrane. Therefore, these experiments reinforce the need for signal recognition to achieve efficient recycling, as previously observed for recycling from the CRE and mediated through AP-1B; in this case, we showed that SNX17 mediates efficient recycling from the BSE.

Notably, IxNPxY-flanking regions A and B are required for binding to SNX17, suggesting that these regions contain elements that support this interaction. Although the exact minimal length of the SNX17-binding domain needs to be determined in the future, it is interesting that both the proximal and distal NPxY motifs in LRP1 bind to SNX17, but only in the presence of regions A and B. This observation suggests the importance of the adjacent sequences, which might enhance the exposure of the motif for SNX17 binding. Through mutagenesis analyses (Figures 2 and 3), we demonstrated that the amino acids adjacent to the IxNPxY motif are critical for the LRP1-SNX17 interaction. Within region B of the SNX17-binding domain, we observed that several acidic residues were required for efficient binding to the IxNPxY motif. These negatively charged amino acids were not observed in residues adjacent to the membrane-distal NPxY motif of LRP1. Notably, this pattern is conserved in other SNX17-binding receptors, including LDLR, LRP1B, ApoER2, and APP. We showed that the acidic residues in this region are critical for interactions with SNX17. The degree of similarity in this region might be correlated with the binding affinity for SNX17. For example, the APP tail shows less similarity to the LRP1 tail, which correlates with its lower binding affinity for SNX17 (data not shown) (7). These observations are additionally supported by the fact that the sequences neighboring the NPxY motifs in the megalin tail show the least similarity and do not support SNX17 binding at these NPxY motifs. In addition, other regions or residues might disrupt binding to SNX17, as the third NPxY motif of megalin tail does not bind to SNX17, although the downstream region of this NPxY motif contains three acidic amino acid residues. To further investigate the effects of region B, we attempted to replace region A with region C. However, this substitution was not successful. Instead, we examined the binding of construct h (Fig. 2), in which region A was replaced with alanines. This construct did not interact with SNX17, indicating that region B alone is not sufficient for this interaction, which requires the support of the appropriate amino acids. Although new evidence related to the interaction of SNX17 with β1-integrin (8, 9) has shown that the membrane distal NPxY motif is flanked at its C-termini by only 3 amino acids, for LRP1the presence of both upstream and downstream regions strengthens the interaction with SNX17, perhaps reflecting a better positioning of the critical residues of the IxNPxY motif.

While LRP1 is unique because it contains two NPxY motifs, which are recognized through distinct adaptor proteins engaged in endocytosis and recycling, many receptors contain only a single NPxY motif that interacts with various adaptor proteins. In fact, the NPxY motifs of LDLR and APP are responsible for both endocytosis and recycling through interactions with completely different adaptor proteins, Dab2 and SNX17, in different cellular compartments, i.e., the plasma membrane and early endosomes, respectively (8, 34). It is not known how these receptors switch between binding to different adaptor proteins in different stages of intracellular trafficking. One attractive possibility is that several of these adaptor proteins compete for binding to a receptor at the cell surface and that their dominance in receptor binding is likely influenced by their relative expression levels and affinity for the receptor. The binding of the adaptor proteins to specific phosphoinositides at the target membrane is

another relevant factor to be considered. For example, Dab2 shows a preference for PtdIns(4,5)P2, enriched at the plasma membrane (40), and SNX17 binds preferentially to PtdIns(3)P (5, 15), which is enriched in the early endosomal compartment. Thus, SNX17 and another PX-FERM protein, SNX27 (41), localized to early endosomes, might bind to the receptor following internalization. The scenario of sequential engagement of adaptor proteins with receptors through their intracellular localization has been recently proposed/established for the binding of kindlin and SNX17 to the distal NPxY motif of β1-integrin at the cell surface and early endosome, respectively (9, 10). Ghai et al. (4) showed that in addition to SNX17, two other sorting nexins, containing PX-FERM domains, SNX27 and SNX31, share the ability to bind the NPxY sorting signals of some common receptors. In addition, these authors highlighted the importance of coincident detection mechanisms (based on sorting signals and the membrane lipid composition) in explaining the sequential engagement of the receptor with different adaptor proteins. We further propose that, in addition to the intracellular localization of receptors, the properties of the amino acids adjacent to a binding motif could specify preferential interactions with specific adaptor proteins. This changing view of protein trafficking suggests that the regulation of receptor trafficking is delicately balanced and that subtle cellular changes might alter the fate of membrane proteins, leading to pathophysiological changes. Identification of the domains of a receptor tail that are both necessary and sufficient for binding to specific adaptor proteins will facilitate the targeting of specific steps of receptor trafficking for therapeutic intervention.

Materials and Methods

Antibodies and reagents

DMEM, L-glutamine, penicillin-streptomycin, and trypsin were purchased from Gibco (Life Technologies Inc., Grand Island, NY, USA). Fetal bovine serum (FBS) was obtained from Hyclone (South Logan, UT, USA). Individual protease inhibitors, puromycin, and all chemical reagents were purchased from Sigma (Sigma Chemical, St Louis MO, USA). Tissue culture-treated Transwell polycarbonate filters were obtained from Costar (Costar, Cambridge, MA). Human recombinant RAP was expressed in a glutathione S-transferase (GST) expression vector and isolated as previously described (35). GST-GFP-RAP was constructed as previously described (33). The monoclonal anti-HA antibody used here has also been previously described (32). A polyclonal anti-SNX17 antibody was raised against a 14-amino acid peptide corresponding to the carboxyl-terminal region of the SNX17 protein, as previously described (8). Human serum with reactivity against EEA1 was obtained as described elsewhere (29). A mouse anti-E-cadherin monoclonal antibody was purchased from BD Biosciences-Pharmingen (San Jose, CA, USA). A mouse anti-transferrin receptor antibody was obtained from Zymed (South San Francisco, CA, USA). An anti-myc antibody (9E10) was obtained from Sigma (St. Louis, MO). Chicken polyclonal anti-HA antibodies were purchased from Chemicon International (Temecula, CA, USA). Anti-Actin and peroxidase-labeled antibodies were obtained from Chemicon (Temecula, CA, USA), and TRITC-conjugated goat-anti-human IgG was purchased from Sigma Chemical. All Alexa-conjugated antibodies were purchased from Molecular Probes (Europe BV, Leiden, the Netherlands), as was Hoechst 33342. EZ-link Sulfo-NHS-LC-biotin, and Immunopure streptavidin-agarose were obtained from Pierce Biochemical (Rockford, IL). Protein A-agarose was purchased from Repligen (Waltham, MA). [^{35}S] methionine/cysteine was obtained from PerkinElmer (Boston, USA). Immobilon-P transfer membranes were obtained from Millipore (Billerica, MA, USA). The ECL System was obtained from Pierce (Rockwell, USA).

Plasmids and fusion proteins

The cytoplasmic domain of mouse LRP1 cloned into the pGEX-2T vector has been described previously (42). Serial deletion and domain swap mutants of GST-LRP1 tail constructs were generated through site-directed mutagenesis using the QuikChange Site-Directed Mutagenesis kit (Stratagene, La Jolla, CA). The megalin minireceptor tagged with the HA epitope (mMeg-1) and the cytoplasmic domain of megalin subcloned into the pGEX-2T vector (GST-MegT) have been previously described (23). mLRP1 and the plasmid encoding RAP have been previously described (35). The wild-type or mutant (Y to A) SNX17-binding cluster of LRP1 was introduced into the GST-Meg tail and mMeg-1 constructs through site-directed mutagenesis using the QuikChange Site-Directed Mutagenesis kit. All constructs were verified through sequencing. The GST fusion proteins were produced in the *Escherichia coli* BL21 strain (Novagen, San Diego, CA) and purified as previously described (42). Dr. Alexis Gautreau (Centre de Recherche de Gif,CNRS, France) provided Rab4-mCherry.

Cell culture and transfection

HEK293 cells were maintained in DMEM containing 10% fetal bovine serum (FBS) (Sigma) and L-glutamine (Invitrogen). The human glioblastoma U87 stable cell line expressing mycSNX17 was maintained in DMEM containing 10% FBS, L-glutamine, sodium pyruvate, and G418 (43). Madin-Darby canine kidney (MDCK) cells (strain II) were maintained in DMEM supplemented with 7.5% fetal bovine serum. All of the cells were cultured in media containing 100 U/ml penicillin and 100 mg/ml streptomycin sulfate.

Clonal cell lines expressing the megalin minireceptors were derived from MDCK cells stably transfected with 2 μg of DNA using the Lipofectamine Plus transfection reagent (Invitrogen) according to the manufacturer's protocol, followed by 10–14 d of selection with 0.8 mg/ml G418 (Invitrogen). The cells were screened and analyzed through Western blotting as described below. The selected clones (at least three for each construct) were maintained in the same medium containing 0.4 mg/ml G418. To achieve transient transfection of cells grown on filters, MDCK cells stably expressing control pLKO or pLKO-shRNA directed against SNX17 were plated on 6.5-mm Transwell filters (0.4-μm pore size) at a density of 5,000 cells per filter. After 2 days, the medium was aspirated and replaced with DMEM without $CaCl_2$ (Life Technologies) and FBS containing pyruvate and 2 mM glutamine. The cells were cultured for 16 h in this medium. The next day, the cells were transfected using 2 μl of Lipofectamine 2000 (Invitrogen) and 1 μg of DNA (0.5 μg of the minireptor plasmid plus 0.5 μg of the plasmid encoding RAP), diluted in 50 μl of DMEM without $CaCl_2$ on each filter, according to the manufacturer's protocol, and incubated for 4–5 h at 37°C. The cells were used 48 h after transfection for immunofluorescence and colocalization analyses.

Lentivirus preparation and infection

For lentivirus production, HEK293 cells were transfected with pCMVR8.91, VSVg, and pLKO (44, 45) or the corresponding shRNA plasmid in the pLKO vector (Open Biosystems RHS3979-98493075) using the calcium phosphate method. After 48 h the supernatant was collected and used to infect the MDCK and HEK293 cell lines in the presence of 8 μg/mL of polybrene. To produce silenced clonal cell lines, the cells were incubated with 2 μg/mL of puromycin in growth medium for 3 days after infection. As a control, uninfected cells were also incubated with puromycin to verify cell death.

GST pull-down assay

GST fusion proteins expressed in bacteria were incubated with glutathione beads at 4°C overnight. The beads were washed twice with PBS and resuspended in PBS. The U87 stable cell line expressing mycSNX17 was lysed in HUNT buffer (20 mM Tris–HCl pH 8.0, 100 mM NaCl, 1 mM EDTA, 0.5% NP-40, 1 mM PMSF, and 1X Complete protease inhibitor cocktail) and incubated with the same amount of fusion proteins bound to glutathione beads for 2 h at 4°C. After washing, the beads (pellets) and supernatants (1% of the total) were boiled in SDS sample buffer and subjected to Western blotting to detect myc-SNX17.

Western blot analysis

Cells were lysed with lysis buffer (PBS containing 1% Triton X-100, 1 mM PMSF, 1 μg/ml each of pepstatin, antipain, and leupeptin) for 1 h at 4°C. The proteins were then separated in SDS-PAGE gels under reducing conditions and transferred to Immobilon-P membranes (Millipore, Billerica, MA). The membranes were blocked in PBS containing 0.05% Tween 20 and 5% nonfat milk, followed by incubation with the corresponding primary antibody and species-specific secondary antibodies conjugated to HRP. The immunoreactive proteins were detected using the ECL system.

FACS analysis of cell surface expression of receptors

HEK293 cells stably expressing SNX17 shRNA or pLKO (control cells) were transfected with the different minireceptors and grown in 100-mm dishes until reaching 80% confluence. The cells were then detached through incubation with PBS/5 mM EDTA. The cell surface minireceptors were detected using a monoclonal anti-HA antibody, followed by incubation with a goat anti-mouse Alexa-488-conjugated antibody (Molecular Probes, Europe BV, Leiden, the Netherlands). The total amount of receptor expression was assessed in cells previously permeabilized with PBS, 0.05% saponin. The background fluorescence intensity was assessed in the absence of the primary antibody and subtracted. The mean fluorescence values were determined in triplicate using FACScalibur (Beckton & Dickinson), and the data were analyzed using the Weasel program.

Steady-state post-endocytic distribution of minimegalin receptors

HEK293 cells stably expressing pLKO or SNX17 shRNA were transiently transfected with mMeg-1, mMeg-2, and mMeg-3. To evaluate colocalization with Rab4, the cells were also transfected with Rab4-mCherry. The cells were washed twice in cold Hepes-buffered DMEM containing 2% BSA and exposed to GST-RAP (200 μg/ml) for 30 min at 37°C. After washing the cells in the same solution, they were incubated with GFP-GST-RAP (75 μg/ml) for 75 min at 37°C, and the remaining ligand at the surface was removed through incubation with stripping buffer (0.1 M glycine, 0.1 M NaCl pH 3) for 5 min. The cells were then fixed with 4% paraformaldehyde in PBSc and permeabilized with 0.2% Triton X-100 in PBSc. The transferrin receptor was detected using monoclonal anti-transferrin receptor and anti-mouse-Alexa 555 antibodies. Images of the cells were captured using a Leica DM 2000 microscope with a 63× oil immersion lens and analyzed as a function of the distribution of GST-GFP-RAP, classifying each cell as showing a vesicular, vesicular-perinuclear, or perinuclear pattern. In each experiment, 100 cells were counted for each condition. The presented results shown correspond to the average of three independent experiments.

Cell Surface Biotinylation in MDCK Cells

MDCK cells were biotinylated as previously described (23, 32). The cells were seeded on Transwell filters (0.4-μm pore size) at a density of 10^5 cells per filter 5 days before the experiment. Cell surface biotinylation was performed at 4°C. The cell monolayers were

washed in PBSc (PBS containing 1.3 mM calcium and 1 mM magnesium) and biotinylated with sulfo-NHS-LC-biotin (0.5 mg/ml) from either the apical (0.5 ml) or basolateral (1.5 ml) chamber compartment. The chamber not receiving biotin was incubated with PBSc. Incubation of the filters was performed twice for 30 min, and biotin was subsequently quenched twice for 10 min through incubation with 50 mM NH4Cl in PBSc. The cells were lysed in ice-cold lysis buffer (150 mM NaCl, 20 mM Tris, pH 8.0, 5 mM EDTA, 1% Triton X-100, 0.2% BSA, and protease inhibitors), and the biotinylated cell surface proteins were adsorbed onto streptavidin agarose beads for 16 h at 4°C. The beads were then washed, and the biotinylated proteins were analyzed through SDS-PAGE, followed by immunoblotting.

Determination of receptor degradation kinetics and stead-state expression levels via metabolic labeling and immunoprecipitation

HEK293 cells transiently expressing mMeg-1, mMeg-2, or mMeg-3 were incubated twice with depletion medium (DMEM without methionine and cysteine) for 20 min and metabolically labeled with 200 mCi/mL of [^{35}S] methionine/cysteine for 9 h. Subsequently, a fresh 1 h pulse of 100 mCi of [^{35}S] methionine/cysteine was administered, corresponding to time 0, and the cells were then chased for 9 or 18 h in complete medium containing 10-fold increased concentrations of methionine (3 mg/ml) and cysteine (6.5 mg/ml). The cells were lysed, and the receptors were immunoprecipitated overnight with an anti-HA monoclonal antibody. The immune complexes were precipitated with Protein A agarose beads. The immunoprecipitated material was released from the beads under reducing conditions after boiling each sample in Laemmli sample buffer (62.5 mM Tris–HCl, pH 6.8, 2% w/v SDS, 10% v/v glycerol, and 5% β-mercaptoethanol) and subsequently analyzed through SDS–PAGE and autoradiography. The experiments were performed in triplicate, and the SD was calculated for each case.

Immunofluorescence

For immunofluorescence analysis of transfected MDCK cells grown on filters (6.5-mm Transwell filters, 0.4-μm pore size, plated at a density of 5,000 cells per filter until confluence) and transfected HEK293 cells grown on glass coverslips, the cells were fixed with 4% paraformaldehyde in PBSc for 20 min at room temperature and subsequently permeabilized with 0.2% Triton X-100 in PBSc for 10 min at room temperature. The fixed cells were then blocked with 0.2% gelatin in PBSc and incubated successively with the primary and the corresponding secondary antibodies for 30 min at 37°C. The filters and glass coverslips were mounted with Mowiol (Calbiochem, San Diego, CA, USA) and analyzed through confocal microscopy using a laser scanning LSM 510 Zeiss microscope and a 63× oil immersion lens or a Leica DM2000 epifluorescence microscope with a 63× oil immersion lens. The images were processed using Image J 1.43 μ.

Colocalization Analysis

The colocalization of the minireceptors with the early endosomal marker EEA1 was determined in polarized MDCK cells grown on filters. The samples were analyzed through confocal microscopy using a laser scanning Zeiss LSM 510 microscope with a 63× oil immersion lens. The obtained images (1,024 ×1,024) were deconvolved using the nearest neighbor algorithm in Metamorph version 6.0r1 software. The area corresponding to the minireceptors and EEA1 was determined to obtain the percentage of the distribution in a given slice over the total area in all slices (30 slices of 0.15–0.2 μm each). Image J was employed with a minimum particle size of 6 pixels and a constant threshold. Stacks of slices containing more than 95% EEA1 labeling and more than 95% HA labeling (receptor) were used for the analyses. Colocalization was quantified using the JACoP plugin of ImageJ software (http://rsb.info.nih.gov/ij/plugins/track/jacop.htlm). For each condition (n≥10 cells per condition), statistical analysis of the correlation of the fluorescence signals of

minireceptor (green) and EEA1 (red) pixels in a dual-channel image was performed using Mander's coefficient and Van Steensel's approach.

To determine the colocalization of GST-GFP-RAP with Rab4-mCherry in HEK293 cells, the samples were analyzed in a manner similar to the analysis performed for colocalization with EEA1, except that the obtained images were deconvolved using Image J, and the percentage of the distribution of GST-GFP-RAP and Rab4-mCherry was determined in each slice over the total area in all slices. The colocalization analysis was performed in slices with the strongest Rab4.mCherry signal and in stacks of slices containing more than 95% of the mCherry labeling and more than 90% of GST-GFP-RAP in each individual condition ($n \geq 15$ cells per condition).

Supplementary Material

Refer to Web version on PubMed Central for supplementary material.

Acknowledgments

The authors would like to thank Dr. Alexis Gautreau (Laboratoire d'Enzymologie et Biochimie Structurales CNRS – Cedex, France) for providing the Rab4-mCherry plasmid. We thank Lisette Sandoval for her collaboration in the SNX17 silencing in MDCK cells. This work was supported through funding from the Fondo Nacional de Ciencia y Tecnología, FONDECYT, grant # 1110382 and the Millenium Nucleus in Regenerative Biology (MINREB), P-07–011-F to MPM and National Institutes of Health grants P01 AG030128 (Project 3) and R01 AG035355 to GB.

References

1. Haft CR, de la Luz Sierra M, Barr VA, Haft DH, Taylor SI. Identification of a family of sorting nexin molecules and characterization of their association with receptors. Mol Cell Biol. 1998; 18(12):7278–7287. [PubMed: 9819414]
2. Seet LF, Hong W. The Phox (PX) domain proteins and membrane traffic. Biochim Biophys Acta. 2006; 1761(8):878–896. [PubMed: 16782399]
3. Worby CA, Dixon JE. Sorting out the cellular functions of sorting nexins. Nat Rev Mol Cell Biol. 2002; 3(12):919–931. [PubMed: 12461558]
4. Ghai R, Bugarcic A, Liu H, Norwood SJ, Skeldal S, Coulson EJ, Li SS, Teasdale RD, Collins BM. Structural basis for endosomal trafficking of diverse transmembrane cargos by PX-FERM proteins. Proc Natl Acad Sci U S A. 2013; 110(8):E643–652. [PubMed: 23382219]
5. van Kerkhof P, Lee J, McCormick L, Tetrault E, Lu W, Schoenfish M, Oorschot V, Strous GJ, Klumperman J, Bu G. Sorting nexin 17 facilitates LRP recycling in the early endosome. Embo J. 2005; 24(16):2851–2861. [PubMed: 16052210]
6. Burden JJ, Sun XM, Garcia AB, Soutar AK. Sorting motifs in the intracellular domain of the low density lipoprotein receptor interact with a novel domain of sorting nexin-17. J Biol Chem. 2004; 279(16):16237–16245. [PubMed: 14739284]
7. Stockinger W, Sailler B, Strasser V, Recheis B, Fasching D, Kahr L, Schneider WJ, Nimpf J. The PX-domain protein SNX17 interacts with members of the LDL receptor family and modulates endocytosis of the LDL receptor. Embo J. 2002; 21(16):4259–4267. [PubMed: 12169628]
8. Lee J, Retamal C, Cuitino L, Caruano-Yzermans A, Shin JE, van Kerkhof P, Marzolo MP, Bu G. Adaptor protein sorting nexin 17 regulates amyloid precursor protein trafficking and processing in the early endosomes. J Biol Chem. 2008; 283(17):11501–11508. [PubMed: 18276590]
9. Steinberg F, Heesom KJ, Bass MD, Cullen PJ. SNX17 protects integrins from degradation by sorting between lysosomal and recycling pathways. J Cell Biol. 2012; 197(2):219–230. [PubMed: 22492727]
10. Bottcher RT, Stremmel C, Meves A, Meyer H, Widmaier M, Tseng HY, Fassler R. Sorting nexin 17 prevents lysosomal degradation of beta1 integrins by binding to the beta1-integrin tail. Nat Cell Biol. 2012; 14(6):584–592. [PubMed: 22561348]

11. Dell'Angelica EC. Clathrin-binding proteins: got a motif? Join the network! Trends Cell Biol. 2001; 11(8):315–318. [PubMed: 11489622]
12. Maurer ME, Cooper JA. The adaptor protein Dab2 sorts LDL receptors into coated pits independently of AP-2 and ARH. J Cell Sci. 2006; 119(Pt 20):4235–4246. [PubMed: 16984970]
13. Borg JP, Ooi J, Levy E, Margolis B. The phosphotyrosine interaction domains of X11 and FE65 bind to distinct sites on the YENPTY motif of amyloid precursor protein. Mol Cell Biol. 1996; 16(11):6229–6241. [PubMed: 8887653]
14. Gallagher H, Oleinikov AV, Fenske C, Newman DJ. The adaptor disabled-2 binds to the third psi xNPxY sequence on the cytoplasmic tail of megalin. Biochimie. 2004; 86(3):179–182. [PubMed: 15134832]
15. Knauth P, Schluter T, Czubayko M, Kirsch C, Florian V, Schreckenberger S, Hahn H, Bohnensack R. Functions of sorting nexin 17 domains and recognition motif for P-selectin trafficking. J Mol Biol. 2005; 347(4):813–825. [PubMed: 15769472]
16. Sheff DR, Daro EA, Hull M, Mellman I. The receptor recycling pathway contains two distinct populations of early endosomes with different sorting functions. J Cell Biol. 1999; 145(1):123–139. [PubMed: 10189373]
17. Bishop NE. Dynamics of endosomal sorting. Int Rev Cytol. 2003; 232:1–57. [PubMed: 14711115]
18. Sannerud R, Saraste J, Goud B. Retrograde traffic in the biosynthetic-secretory route: pathways and machinery. Curr Opin Cell Biol. 2003; 15(4):438–445. [PubMed: 12892784]
19. Hsu VW, Prekeris R. Transport at the recycling endosome. Curr Opin Cell Biol. 2010; 22(4):528–534. [PubMed: 20541925]
20. Jovic M, Sharma M, Rahajeng J, Caplan S. The early endosome: a busy sorting station for proteins at the crossroads. Histol Histopathol. 2010; 25(1):99–112. [PubMed: 19924646]
21. Chia PZ, Gleeson PA. The regulation of endosome-to-Golgi retrograde transport by tethers and scaffolds. Traffic. 2011; 12(8):939–947. [PubMed: 21477175]
22. Nagai M, Meerloo T, Takeda T, Farquhar MG. The adaptor protein ARH escorts megalin to and through endosomes. Mol Biol Cell. 2003; 14(12):4984–4996. [PubMed: 14528014]
23. Yuseff MI, Farfan P, Bu G, Marzolo MP. A cytoplasmic PPPSP motif determines megalin's phosphorylation and regulates receptor's recycling and surface expression. Traffic. 2007; 8(9): 1215–1230. [PubMed: 17555532]
24. Lauffer BE, Melero C, Temkin P, Lei C, Hong W, Kortemme T, von Zastrow M. SNX27 mediates PDZ-directed sorting from endosomes to the plasma membrane. J Cell Biol. 2010; 190(4):565–574. [PubMed: 20733053]
25. Gan Y, McGraw TE, Rodriguez-Boulan E. The epithelial-specific adaptor AP1B mediates post-endocytic recycling to the basolateral membrane. Nat Cell Biol. 2002; 4(8):605–609. [PubMed: 12105417]
26. Lock JG, Stow JL. Rab11 in recycling endosomes regulates the sorting and basolateral transport of E-cadherin. Mol Biol Cell. 2005; 16(4):1744–1755. [PubMed: 15689490]
27. Gravotta D, Deora A, Perret E, Oyanadel C, Soza A, Schreiner R, Gonzalez A, Rodriguez-Boulan E. AP1B sorts basolateral proteins in recycling and biosynthetic routes of MDCK cells. Proc Natl Acad Sci U S A. 2007; 104(5):1564–1569. [PubMed: 17244703]
28. Carvajal-Gonzalez JM, Gravotta D, Mattera R, Diaz F, Bay AP, Roman AC, Schreiner RP, Thuenauer R, Bonifacino JS, Rodriguez-Boulan E. Basolateral sorting of the coxsackie and adenovirus receptor through interaction of a canonical YXXPhi motif with the clathrin adaptors AP-1A and AP-1B. Proc Natl Acad Sci U S A. 2012; 109(10):3820–3825. [PubMed: 22343291]
29. Donoso M, Cancino J, Lee J, van Kerkhof P, Retamal C, Bu G, Gonzalez A, Caceres A, Marzolo MP. Polarized traffic of LRP1 involves AP1B and SNX17 operating on Y-dependent sorting motifs in different pathways. Mol Biol Cell. 2009; 20(1):481–497. [PubMed: 19005208]
30. Wilson JM, de Hoop M, Zorzi N, Toh BH, Dotti CG, Parton RG. EEA1, a tethering protein of the early sorting endosome, shows a polarized distribution in hippocampal neurons, epithelial cells, and fibroblasts. Mol Biol Cell. 2000; 11(8):2657–2671. [PubMed: 10930461]
31. Sheff DR, Kroschewski R, Mellman I. Actin dependence of polarized receptor recycling in Madin-Darby canine kidney cell endosomes. Mol Biol Cell. 2002; 13(1):262–275. [PubMed: 11809838]

32. Marzolo MP, Yuseff MI, Retamal C, Donoso M, Ezquer F, Farfan P, Li Y, Bu G. Differential distribution of low-density lipoprotein-receptor-related protein (LRP) and megalin in polarized epithelial cells is determined by their cytoplasmic domains. Traffic. 2003; 4(4):273–288. [PubMed: 12694565]
33. Vicinanza M, Di Campli A, Polishchuk E, Santoro M, Di Tullio G, Godi A, Levtchenko E, De Leo MG, Polishchuk R, Sandoval L, Marzolo MP, De Matteis MA. OCRL controls trafficking through early endosomes via PtdIns4,5P(2)-dependent regulation of endosomal actin. EMBO J. 2011; 30(24):4970–4985. [PubMed: 21971085]
34. Morris SM, Cooper JA. Disabled-2 colocalizes with the LDLR in clathrin-coated pits and interacts with AP-2. Traffic. 2001; 2(2):111–123. [PubMed: 11247302]
35. Li Y, Marzolo MP, van Kerkhof P, Strous GJ, Bu G. The YXXL motif, but not the two NPXY motifs, serves as the dominant endocytosis signal for low density lipoprotein receptor-related protein. J Biol Chem. 2000; 275(22):17187–17194. [PubMed: 10747918]
36. Roque AC, Lowe CR. Lessons from nature: On the molecular recognition elements of the phosphoprotein binding-domains. Biotechnol Bioeng. 2005; 91(5):546–555. [PubMed: 15959902]
37. Folsch H, Pypaert M, Schu P, Mellman I. Distribution and function of AP-1 clathrin adaptor complexes in polarized epithelial cells. J Cell Biol. 2001; 152(3):595–606. [PubMed: 11157985]
38. Ang AL, Folsch H, Koivisto UM, Pypaert M, Mellman I. The Rab8 GTPase selectively regulates AP-1B-dependent basolateral transport in polarized Madin-Darby canine kidney cells. J Cell Biol. 2003; 163(2):339–350. [PubMed: 14581456]
39. Henry L, Sheff DR. Rab8 regulates basolateral secretory, but not recycling, traffic at the recycling endosome. Mol Biol Cell. 2008; 19(5):2059–2068. [PubMed: 18287531]
40. Mishra SK, Keyel PA, Hawryluk MJ, Agostinelli NR, Watkins SC, Traub LM. Disabled-2 exhibits the properties of a cargo-selective endocytic clathrin adaptor. EMBO J. 2002; 21(18):4915–4926. [PubMed: 12234931]
41. Lunn ML, Nassirpour R, Arrabit C, Tan J, McLeod I, Arias CM, Sawchenko PE, Yates JR 3rd, Slesinger PA. A unique sorting nexin regulates trafficking of potassium channels via a PDZ domain interaction. Nat Neurosci. 2007; 10(10):1249–1259. [PubMed: 17828261]
42. Bu G, Geuze HJ, Strous GJ, Schwartz AL. 39 kDa receptor-associated protein is an ER resident protein and molecular chaperone for LDL receptor-related protein. Embo J. 1995; 14(10):2269–2280. [PubMed: 7774585]
43. Bu G, Maksymovitch EA, Geuze H, Schwartz AL. Subcellular localization and endocytic function of low density lipoprotein receptor-related protein in human glioblastoma cells. J Biol Chem. 1994; 269(47):29874–29882. [PubMed: 7961982]
44. Fuentealba RA, Liu Q, Kanekiyo T, Zhang J, Bu G. Low density lipoprotein receptor-related protein 1 promotes anti-apoptotic signaling in neurons by activating Akt survival pathway. J Biol Chem. 2009; 284(49):34045–34053. [PubMed: 19815552]
45. Stewart SA, Dykxhoorn DM, Palliser D, Mizuno H, Yu EY, An DS, Sabatini DM, Chen IS, Hahn WC, Sharp PA, Weinberg RA, Novina CD. Lentivirus-delivered stable gene silencing by RNAi in primary cells. RNA. 2003; 9(4):493–501. [PubMed: 12649500]

Synopsis

SNX17 is an early endosomal protein that allows efficient recycling of membrane receptors, such as LRP1 and LDLR, containing an NPxY motif in the cytoplasmic domain. When expressed in polarized epithelial cells, both receptors distribute basolaterally and recycle through the basolateral sorting endosome (BSE). This study describes in detail the SNX17-binding domain present in the LRP1's cytoplasmic domain and demonstrates that in polarized epithelial cells the function of SNX17 is restricted to the basolateral cargo recycling through the BSE.

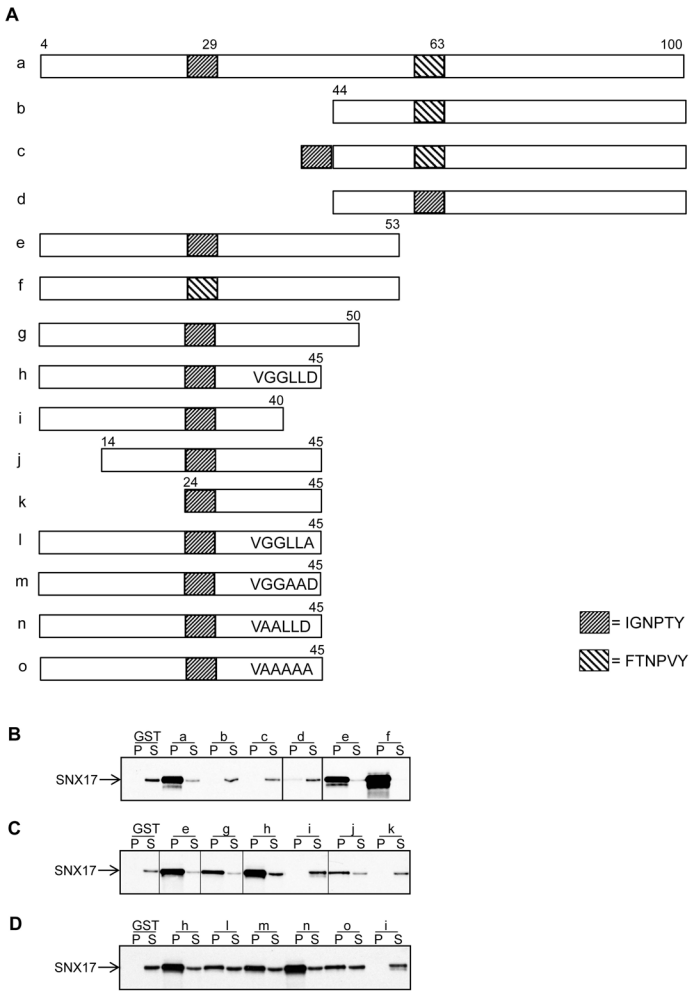

Figure 1.

The IxNPxY motif is not sufficient for binding to SNX17 (A). Schematic diagrams of the wild-type and mutant LRP1 tails. Residue number 4 is the fourth amino acid following the transmembrane domain. The two NPxY motifs are indicated. Construct “a” depicts the full-length LRP1 tail. The N-terminal half of the LRP1 tail (construct “e”) binds to SNX17, but the C-terminal half of the LRP1 tail (construct “b”) does not. The IxNPxY motif was added upstream of T44-100 (construct “c”) or replaced in the C-terminal half (construct “d”). The FTNPVY motif was replaced in the N-terminal half (construct “f”). The N-terminal half with serial deletion mutations (“g–k”) and mutants with substitutions of the last 5 amino acids (constructs “l–o”) are also shown (B). GST pull-down assays. Equal amounts of GST fusion proteins were incubated with lysates from the U87 stable cell line expressing mycSNX17. “P” and “S” indicate the pellet (beads) and the supernatant (1%) fractions, respectively, after incubation with the lysates in all figures. The bound proteins were detected using the antimyc antibody. GST alone served as a negative control. (C). GST pull-down assays of GST fusion proteins of LRP1 tails with serial deletion mutations. (D) GST pull-down assays of GST fusion proteins of LRP1 tails containing alanine mutations.

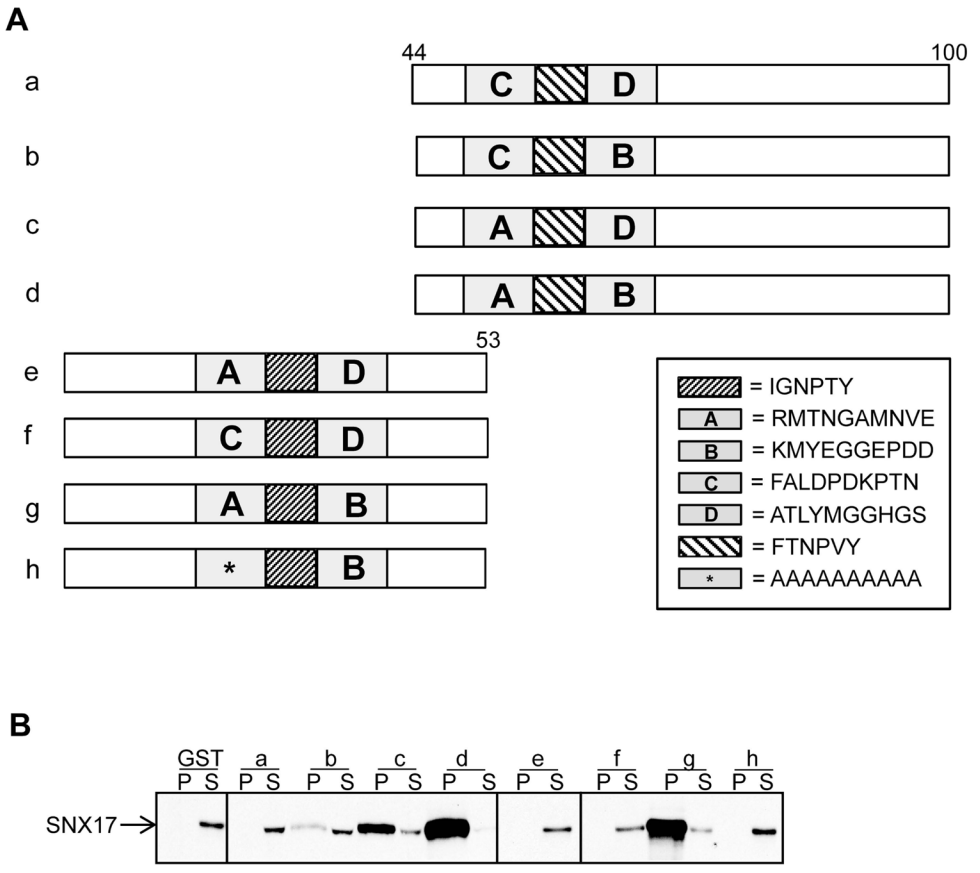

Figure 2.

Amino acids adjacent to the IGNPTY motif are required for binding of LRP1 to SNX17. (A). Schematic diagrams of the wild-type and mutant C-terminal and N-terminal regions (T44-100 and T4-53, respectively) of the LRP1 tails. The IGNPTY and FTNPVY motifs are indicated as in Figure 1A. The upstream and downstream regions of the IxNPxY or FxNPxY motifs are shown in the gry boxes labeled A through D. (B). GST pull-down assays using the constructs depicted in A.

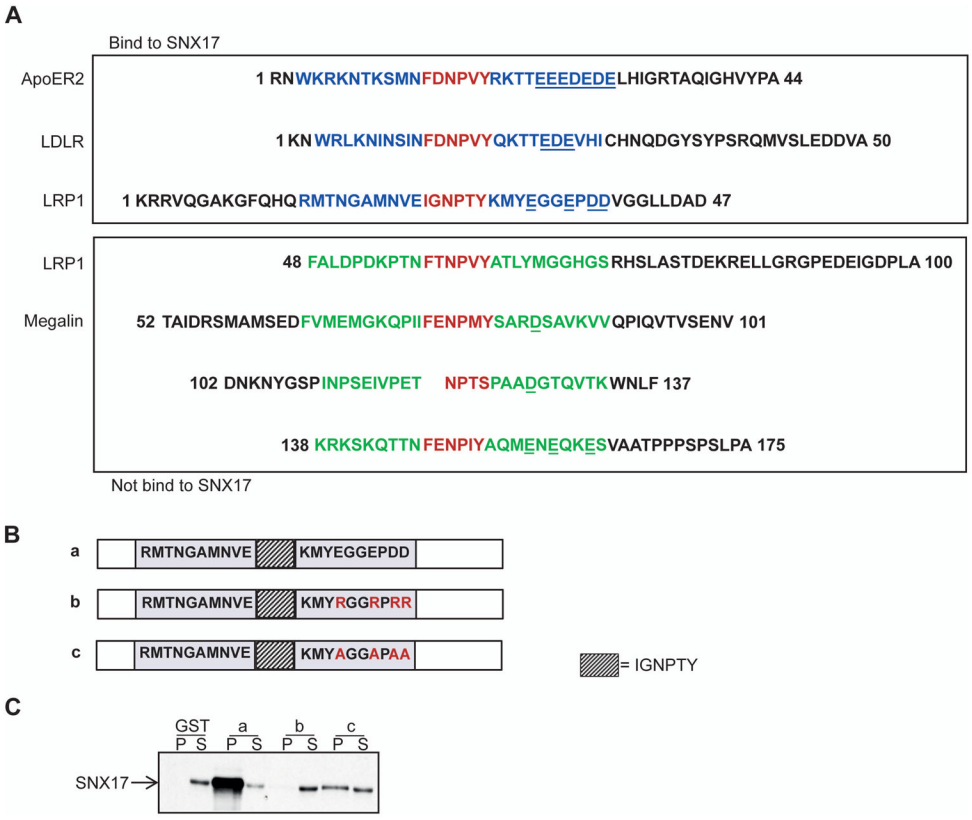

Figure 3.

Acidic amino acids downstream of the IGNPTY motif are critical for LRP1 binding to SNX17. (A). Amino acid alignments of the SNX17-binding receptor tails (ApoER2, LDLR, and N-terminal half of LRP1) and non-binding receptor tails, megalin, and the C-terminal half of LRP1. The NPxY motifs are indicated in red, and the adjacent residues are indicated in blue for the binding receptors and green for the non-binding receptors. (B). Schematic diagram of the wild-type (a) and mutant N-terminal half of the LRP1 tails ("b" and "c"). The NPxY motif is indicated as in Figure 1A. The gray boxes indicate the 10 amino acids from the upstream and downstream regions of the NPxY motif. The mutated or substituted residues are shown in red. (C) GST pull-down assays using the wild-type and mutant LRP1 tails (b and c) depicted in B show that mutation of the negatively charged amino acids downstream of the NPVY motif disrupts interactions with SNX17.

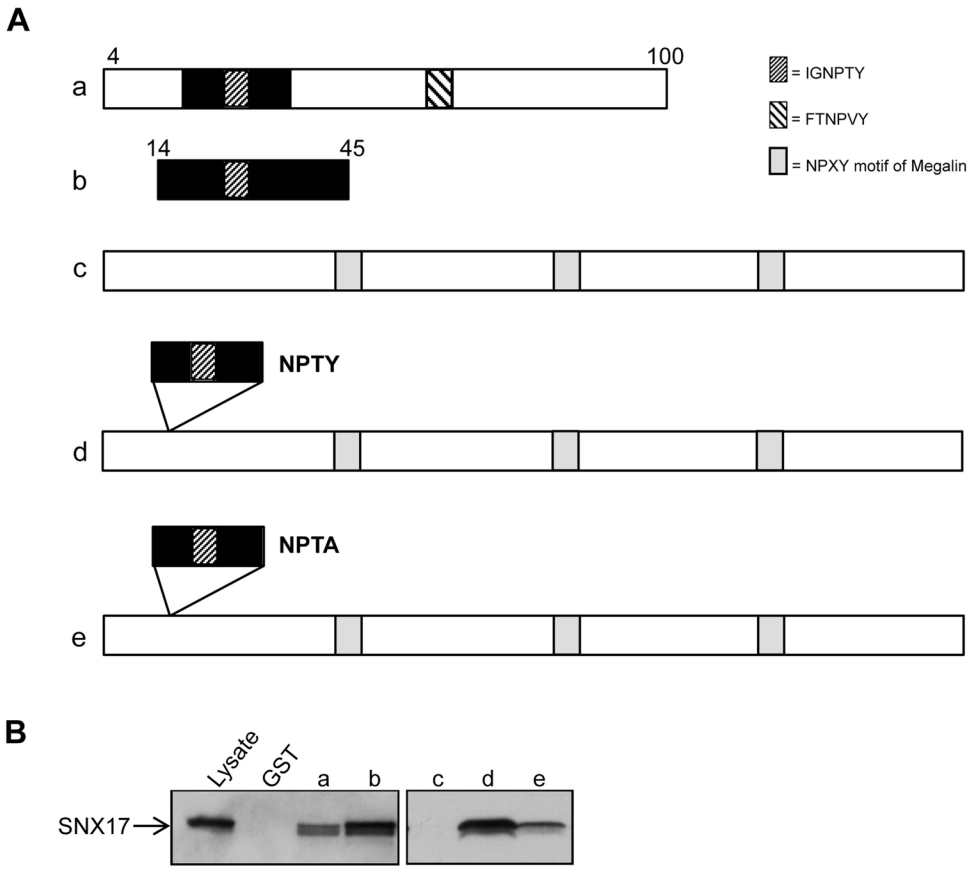

Figure 4.

The megalin chimeric receptor containing the SNX17 binding domain of LRP1 interacts with SNX17. (A) Schematic diagrams of the cytoplasmic domains of LRP1 (full-length tail of 100 amino acids and T14-45, constructs “a” and “b”, respectively) and megalin (wild-type, full-length tail, 209-amino acid construct “c” and chimeras “d–e”). Residue number 4 is the fourth amino acid following the transmembrane domain of the LRP1 tail. Constructs “d” and “e” correspond to megalin tails containing the wild-type or mutant SNX17-binding domain, respectively, after the thirteenth amino acid following the transmembrane domain. The tail proteins were fused to GST. The mutant SNX17-binding domain contains a Y to A mutation. (B) GST pull-down assays using the megalin tail constructs containing the wild-type and mutant SNX17-binding domain. GST serves as a negative control and GST-LRP1 tail (full-length) and T14-45 were the positive controls. The presence of the SNX17-binding domain within the megalin tail (as shown in construct “d”) supports its binding to SNX17.

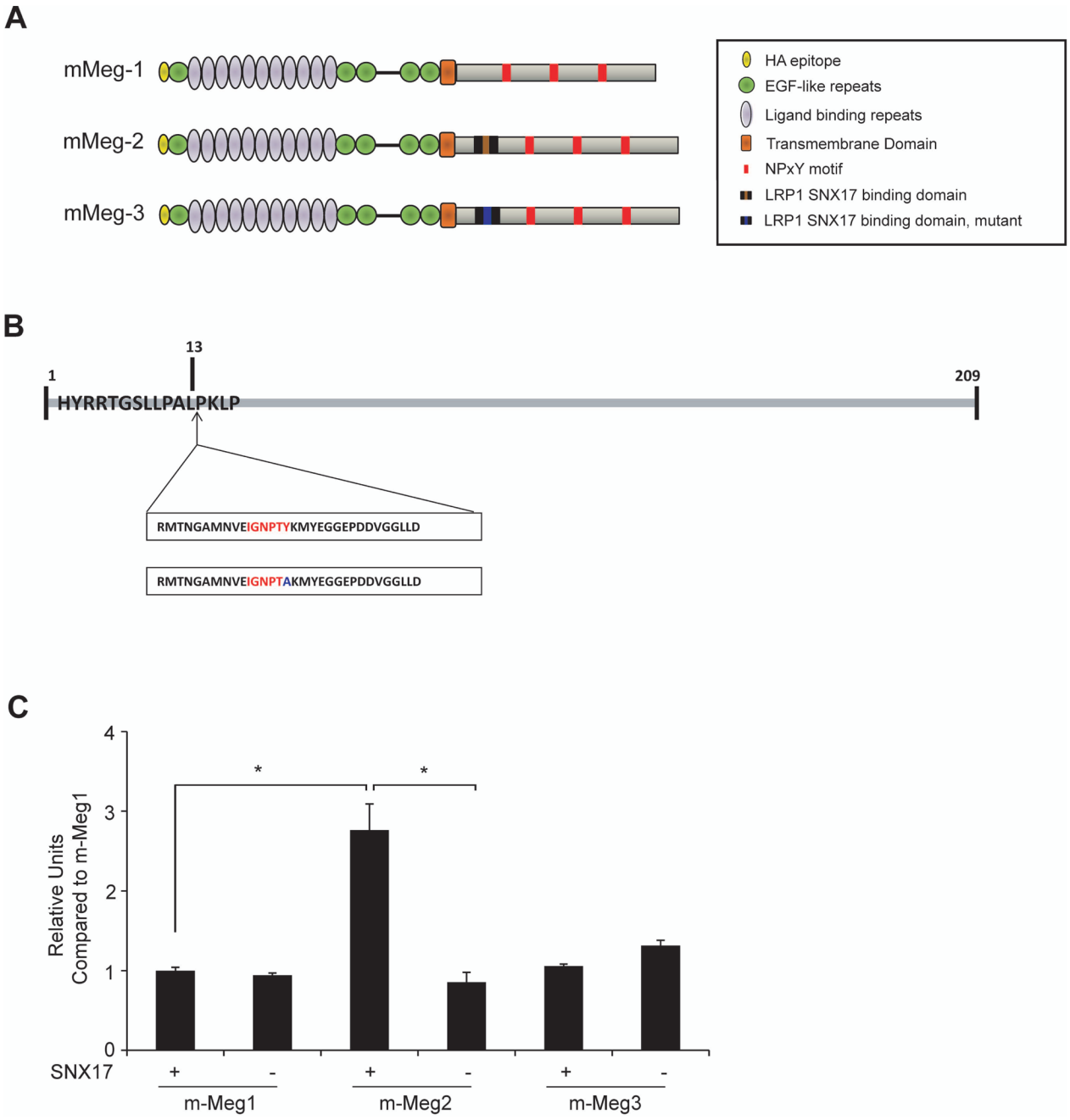

Figure 5.

The presence of the SNX17-binding domain or LRP1 in the megalin tail increases the expression of the chimeric receptor at the cell surface. (A) Schematic representation of megalin minireceptors. The sequences shown in B, corresponding to the native or mutated SNX17-binding domain of LRP1, were inserted proximal to the transmembrane domain of megalin, generating the constructs mMeg-2 and mMeg-3, respectively. mMeg-1 is a megalin minireceptor that harbors the fourth ligand-binding domain and the transmembrane and cytoplasmic domains of megalin (23) (B) Sequences of the SNX17-binding domain of LRP1 and the point of insertion within the megalin cytoplasmic domain. (C) Control or SNX17 KD HEK293 cells were transiently transfected with the minireceptors mMeg-1, mMeg-2,

and mMeg-3. The cells (either intact or permeabilized with 0.05% saponin) were then incubated with anti-HA and Alexa-488-conjugated anti-mouse IgG and analyzed through flow cytometry. The results are plotted as the ratio of the minimegalin expression levels observed in intact versus permeabilized cells. The assays were performed in triplicate, and the averages ± SD are plotted in the graph (*$p < 0.01$ versus mMeg-1).

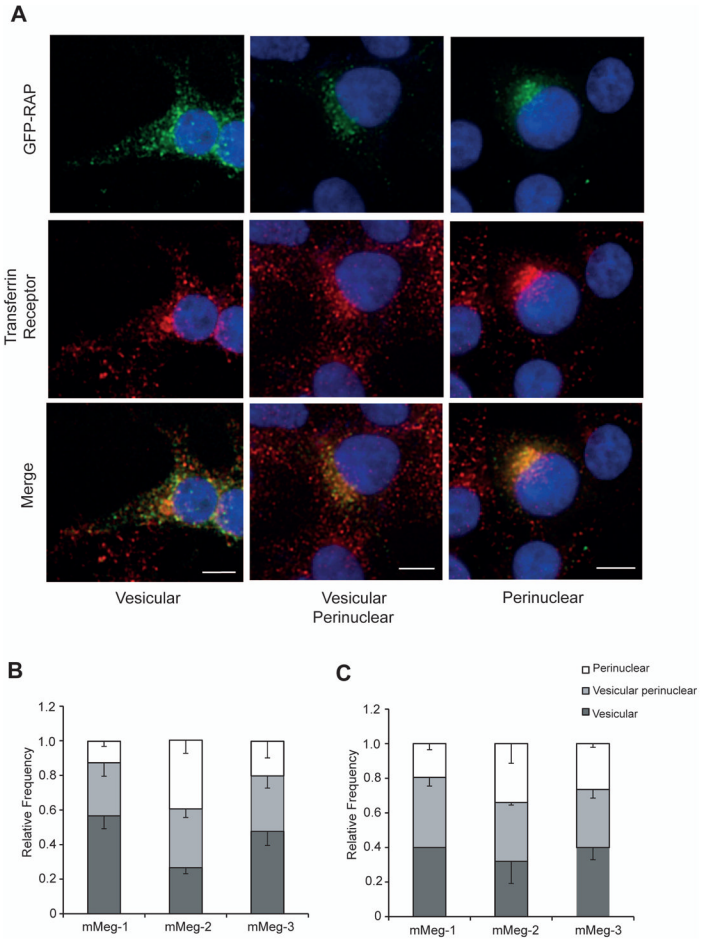

Figure 6.

The presence of the SNX17-binding domain within the megalin tail changes the postendocytic distribution of the receptor. Control or SNX17 KD HEK293 cells were transfected with mMeg-1, mMeg-2, or mMeg-3. The cells were then incubated with GST-RAP (200 μg/μl) at 37°C for 30 min, followed by GST-GFP-RAP (75 μg/μl) at 37°C for 75 min. (A) The distribution of GST-GFP-RAP was determined for all cells, and three frequent, clearly visible patterns were defined in this analysis: vesicular, vesicular with a perinuclear component, and predominant perinuclear distributions. The nuclei were visualized using Hoechst staining. TfR was enriched in the perinuclear region, corresponding to a recycling compartment, and colocalizes with the perinuclear distribution of the internalized GST-GFP-RAP. Scale bars: 5 μm. (B) Quantification of the cellular phenotypes of the minireceptor/ligand distribution observed for HEK293 control cells, or (C) cells expressing shRNA directed against SNX17. The distribution of mMeg-2/GST-GFP-RAP is significantly more perinuclear than the distribution of mMeg-1 and mMeg-3 in cells expressing SNX17 (B), but not in cells devoid of the adaptor (C). The results shown in the graphs were derived from three experiments, with 100 cells analyzed under each experimental condition. The averages ± SD are plotted in the graph. See Table S1 for the numerical data.

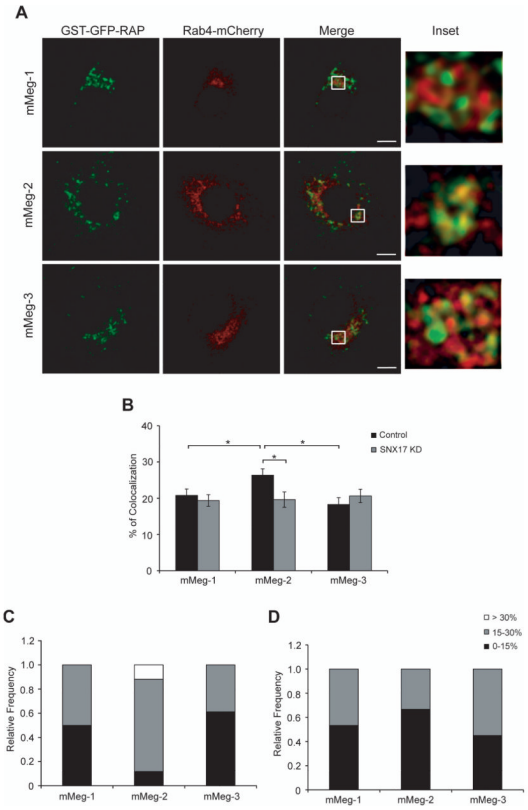

Figure 7.

Colocalization of minireceptors with Rab4-recycling endosomes. Control or SNX17 KD HEK293 cells, transfected with mMeg-1, mMeg-2, mMeg-3, and Rab4-mCherry, were incubated with GST-RAP (200 μg/μl) for 30 min, followed by GST-GFP-RAP (75 μg/μl) for 75 min. (A) Confocal images corresponding to the control cells showing the colocalization of Rab4 and the receptors. Scale bar, 5 μm. (B) The percentages of Rab4-mCherry and GST-GFP-RAP colocalization in control and SNX17 KD cells expressing the minireceptors are plotted in the graph (*$p < 0.05$; average ± SE, $n > 15$ cells). The analysis was conducted in the confocal section exhibiting the strongest Rab4-mCherry signal. (C) The distribution of the quantified percentages of GST-GFP-RAP/ Rab4-mCherry colocalization obtained from the confocal stacks of HEK293 control cells or (D) SNX17-silenced cells.

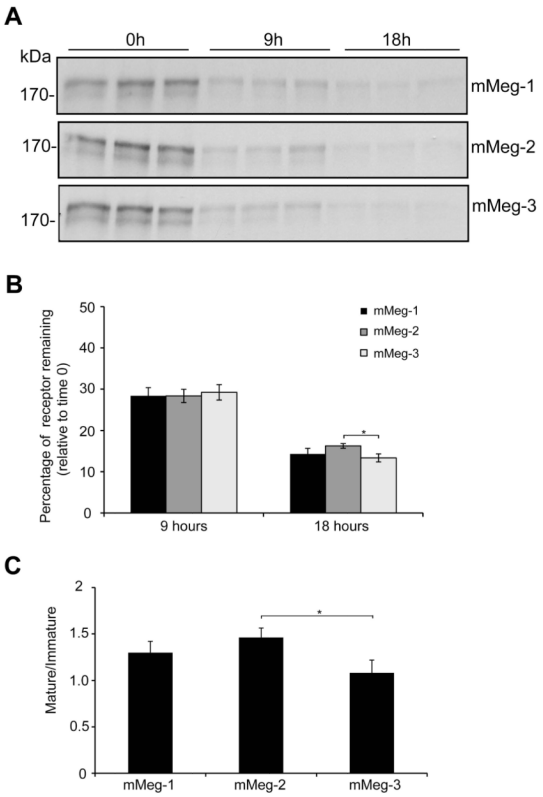

Figure 8.

Effect of the SNX17-binding domain on the half-life of megalin. (A) HEK293 cells transiently expressing m-Meg1, m-Meg2, and m-Meg3 were metabolically labeled with [35S] methione/cysteine and chased for different times. The minireceptors were immunoprecipitated from the cell lysates using an anti-HA antibody and analyzed via 5% SDS–PAGE (B) Quantification of the radiolabeled proteins (mature band, high molecular weight) showed that m-Meg2 is significantly more stable than m-Meg3 after 18 hours of chase, although the difference was small. The levels of the minireceptors after 9 hours were similar. (C) Quantification of the ratio between the mature/immature bands at time 0 indicated that m-Meg2 shows slightly more stable expression compared with m-Meg3. The assay was performed in triplicate, and the averages ± SD are plotted in the graph (*$p < 0.05$).

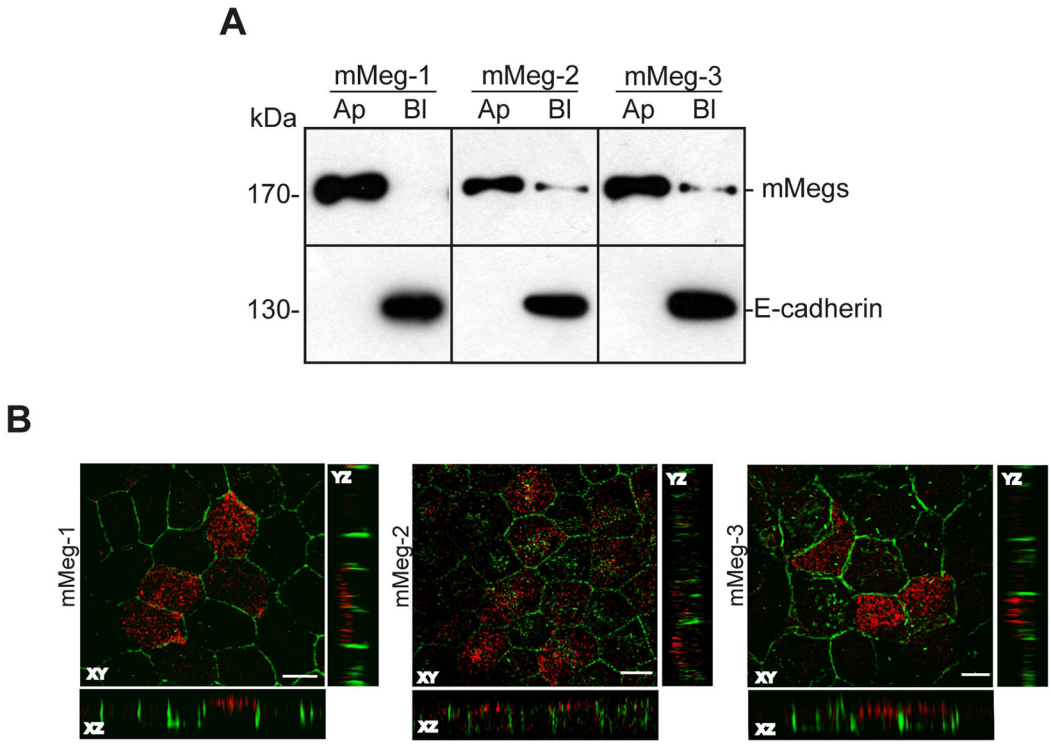

Figure 9.

The polarized cell surface distribution of mMeg is not modified by the presence of the SNX17-binding domain of LRP1. The cell surface distribution of mMeg-1, mMeg-2, and mMeg-3 was determined in MDCK cell lines stably expressing the minimegalins. The cells were grown until forming an impermeable monolayer in Transwell chambers. (A) The cells were then selectively biotinylated at 4°C, and the cell lysates were analyzed via Western blotting. All the minireceptors were localized apically. The membrane was stripped and blotted to detect the endogenous protein E-cadherin, showing correct basolateral localization. (B) Polarized MDCK cells expressing mMeg-1, mMeg-2, and mMeg-3 were grown on Transwell filters to analyze the localization of the minireceptors through immunofluorescence and confocal microscopy. The cells were fixed, permeabilized, and incubated with anti-HA (red), to detect the minireceptors, and mouse anti-E-cadherin (green), to determine the endogenous lateral marker. The minireceptors show a predominant apical localization. Representative x–y plane and x–z and y–z sections are shown. Scale bars, 10 μm.

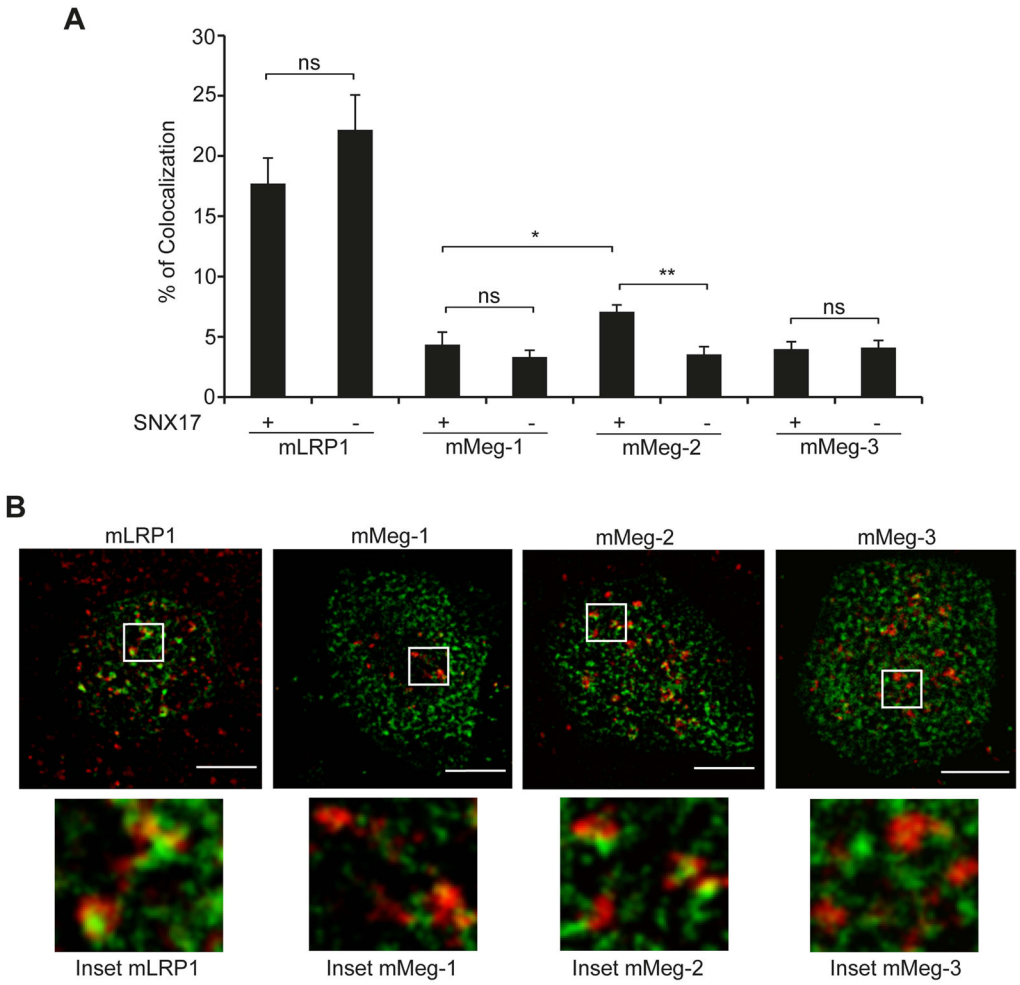

Figure 10.

Presence of minireceptors in EEA1 endosomes in polarized MDCK cells. Control or SNX17 KD MDCK cells were grown on filters until polarization was achieved and then transfected for transient expression of mLRP1, mMeg-1, mMeg-2, and mMeg-3. The cells were processed for immunofluorescence to detect the total HA-tagged minireceptors and the early endosome marker EEA1. (A) The percentages of colocalization are plotted in the graph and show that mMeg-2 shows significantly more co-localization with EEA1 than mMeg-1 (*$p < 0.05$) in cells expressing SNX17 and that this co-localization is SNX17 dependent (**$p < 0.01$ vs. mMeg-2 in SNX17 KD cells; average ± SE, $n > 10$ cells). (B) Confocal images corresponding to the slices in which both EEA1 (red) and the receptor (green) show maximal expression in control cells. Scale bar, 5 μm.